Chemical Engineering Science 100 (2013) 464–473

Contents lists available at SciVerse ScienceDirect

Chemical Engineering Science

journal homepage: www.elsevier.com/locate/ces

Mass transfer properties in a bubble column associated with micro-bubble dispersions

Katsuhiko Muroyama [a,*], Kouhei Imai [b], Yuji Oka [b], Jun'ichi Hayashi [c]

[a] *Kansai University, 3-3-35 Yamate-cho, Suita City, Osaka 564-8680, Japan*
[b] *Graduate School of Science and Engineering, 3-3-35 Yamate-cho, Suita City, Osaka 564-8680, Japan*
[c] *Department of Chemical, Energy and Environmental Engineering, Kansai University, 3-3-35 Yamate-cho, Suita City, Osaka 564-8680, Japan*

HIGHLIGHTS

- Dispersion of micro-bubbles with diameters $< 50\ \mu m$ verifies a superior gas-absorption performance.
- The self-compression and shrinking effects enhanced the gas absorption from the micro-bubbles.
- The values of kLa were well predicted by the complete absorption model at high dispersion heights.
- Absorption efficiency can be correlated well with the ratio of dispersion height to linear gas velocity.
- Specific interfacial areas were extremely greater than those for conventional dispersion systems.

ARTICLE INFO

Article history:
Received 4 September 2012
Received in revised form
14 March 2013
Accepted 20 March 2013
Available online 4 April 2013

Keywords:
Micro-bubble
Bubble column
Specific interfacial area
Apparent volumetric mass transfer coefficient
Oxygen absorption efficiency
Self-compression and shrinking mechanism

ABSTRACT

The goal of this study was to investigate the gas holdup, bubble size distribution, and Sauter mean diameter for oxygen micro-bubble dispersions in water in an acrylic-acid resin column with an inner diameter of 0.15 m, and with a working liquid height varying from 0.500 to 1.850 m. The micro-bubbles, which varied in their Sauter mean diameters from 32 to 40 μm depending on the gas velocity, were employed to measure their superior mass transfer properties, which are enhanced by the effects of self-compression and shrinking. The apparent liquid-side mass transfer coefficient, k_La, in the micro-bubble column was also measured using the transient absorption from oxygen micro-bubbles into degassed water or into nitrogen-desorbed water. The obtained values of k_La for oxygen absorption into the degassed water were significantly greater than those for absorption into nitrogen-desorbed water. The k_La values for the degassed water were represented well by the complete absorption model, and generally increased with increasing gas flow rate. It was found that the oxygen absorption efficiency, which was defined by the ratio of the absorption rate to the supply rate of oxygen, decreased with increasing gas flow rate and increased with increasing liquid depth. The oxygen absorption efficiency could be described well by an empirical correlation in terms of the ratio of the liquid height to the superficial gas velocity, h/U_G, or in terms of the ratio of the liquid height to the linear gas velocity, $h/(U_G/\varepsilon_G)$.

1. Introduction

Recently, micro-bubble technology has attracted great attention because micro-bubbles exhibit superior characteristics in terms of physical chemistry and size effects, and also have specific functions unlike those of normal milli-bubbles. Important bioactive and growth-promoting effects have already been confirmed for water treatments using micro-bubbles. Micro-bubble technology was developed for the restoration of closed environmental waters such as ponds or dam reservoirs and is widely used in technologies for environmental protection and energy savings (Ohnari, 2007; Tsuge, 2007; Ohnari et al., 2012). Various aspects of micro-bubbles have been investigated by Takahashi and his research group (Takahashi, 2012). The physical properties of micro-bubble dispersions in a bubble column have been investigated (Li and Tsuge, 2006a and 2006b; Muroyama et al., 2012).

In this work, for the purpose of comparison, bubble-size distribution and liquid-side volumetric mass transfer coefficients were measured in milli-bubble dispersion systems at gas flow rates similar to those for the micro-bubble dispersions. A large amount of literature has been published in journals and books describing milli-bubble dispersions in bubble columns. Extensive

---

[*] Corresponding author. Tel.: +88 6 6368 1121; fax: +88 6 6368 8869.
E-mail address: v902362@kansai-u.ac.jp (K. Muroyama).

0009-2509/$ - see front matter © 2013 Elsevier Ltd. All rights reserved.
http://dx.doi.org/10.1016/j.ces.2013.03.043

reviews and a few books are introduced here to describe several aspects related to gas–liquid mass-transfer in milli-bubble dispersion operations (Shah et al., 1982; Muroyama and Fan, 1985; Fan, 1989; Ueyama, 1993).

When considering the industrial applications of micro-bubble technology, it is important to assess the benefits based on scientific principles and from an academic standpoint and to compare micro-bubble technology with existing technology both in terms of its functional quality and effectiveness (Kawabata and Muroyama, 2010; Muroyama et al., 2012b). Thus, it is necessary to describe clearly the superior physical and chemical characteristics of micro-bubbles, particularly those with diameters less than approximately 50 μm, and mass transfer enhancement caused by the self-compression and shrinking of these micro-bubbles, which leads to collapse and complete gas dissolution (Takahashi, 2005; Takahashi et al., 2007b). The remarkable mass transfer properties of a dispersion of shrinking micro-bubbles were found to depend on the ability of these bubbles to self-compress and collapse in the water, leading to the active generation of hydroxyl radicals (Li et al., 2009a and 2009b).

In the present work, the gas holdup, bubble-size distribution, Sauter mean diameter and apparent volumetric mass transfer coefficient, k_La, were measured for oxygen micro-bubble dispersions. These dispersions consisted of uniform micro-bubbles with volume-surface mean diameters less than 50 μm in a column with an inside diameter of 0.15 m with column heights varying from 0.5 to 2.0 m. The values of oxygen absorption efficiency for the micro-bubble dispersions in degassed water were compared with those in nitrogen-desorbed water. Additionally, the properties of the swarm bubbles for a system equipped with a compression-dissolution micro-bubble generator were compared with those for a milli-bubble dispersion system equipped with a porous glass filter nozzle. The goal of the present investigation was to clarify the superiority of micro-bubble dispersions for mass transfer.

2. Experimental apparatus and method

2.1. Experimental apparatus

Fig. 1 shows a schematic diagram of the experimental apparatus used. The experimental column consisted of an acrylic-acid resin pipe of 150 mm ID and a length varying from 500 to 2000 mm. The micro-bubble generator (AS-KS, ASP corporation) used in the experiment was a combination of high-speed-rotation- and compression-dissolution-type generators. Using this generator, an aqueous emulsion of micro-bubbles was discharged into the center of the bottom of the column through a 16-mm ID hole at a rate between 5.0 and 15.0 L/min. Gas from an oxygen or a nitrogen cylinder was introduced into the M–B generator through a mass flow meter, which measured the flow rate. The micro-bubbles were typically supplied with a circulating liquid rate of 10 L/min. The temperature of the liquid in the column was controlled at 25 ± 0.1 °C with a cooling coil through which cooling liquid was circulated from a cooler. To carry out hydrodynamic and mass transfer experiments for milli-bubble dispersions with narrow size distributions at superficial gas flow rates similar to those used in the micro-bubble dispersions, gases from the two previously described cylinders were introduced into the column through a G3 glass filter nozzle fitted at the center of the bottom of the column. Typical experimental conditions are summarized in Table 1.

2.2. Measurement of bubble-size distribution

The size distribution of the micro-bubble dispersions was evaluated using the following method. A sample of oxygen saturated water containing micro-bubbles was withdrawn from the column wall using a small pump and sent into a 6-mm-deep rectangular cell. In this cell, photographs of the swarm bubbles were taken at a magnification of 200 and at a shutter speed of 1/2000 s with a digital micro-scope (VHX-100FN, Keyence Corp.). Such samples were taken repeatedly throughout each experiment. The bubble-size distribution was analyzed using a software program (SigmaScan Pro 5, HULINKS) in which non-overlapping frames of the bubble swarm images were processed to evaluate approximately 1000 volume-equivalent spherical diameters. It was assumed that the bubbles could be modeled as flat rotating ellipsoids that rose along their minor axis (oblate spheroids, as described by Weisstein, 2012). Thus, the volume-equivalent spherical diameter d_{vi} was determined from the major axis l_i and minor axis m_i of each bubble using the following equation:

$$d_{vi} = \sqrt[3]{l_i^2 m_i} \tag{1}$$

After it was confirmed that the micro-bubbles were nearly spherical in shape, the volume-surface mean diameter d_{vs} could be defined. This quantity is based on the volume-equivalent spherical diameter as follows (Muroyama et al., 2012a):

$$d_{vs} = \sum_{i=1}^{n} d_{vi}^3 \Bigg/ \sum_{i=1}^{n} d_{vi}^2 \tag{2}$$

Note that for micro-bubbles that are nearly spherical, the quantity d_{vs} defined by Eq. (2) approximates the Sauter mean diameter, which is the true volume-surface mean diameter for a swarm of non-spherical bubbles.

To take photographs of the milli-bubble dispersions, a 400-mm-long column, outside of which a square tank with sides of 270 mm and a depth of 260 mm was fitted to remove the effects

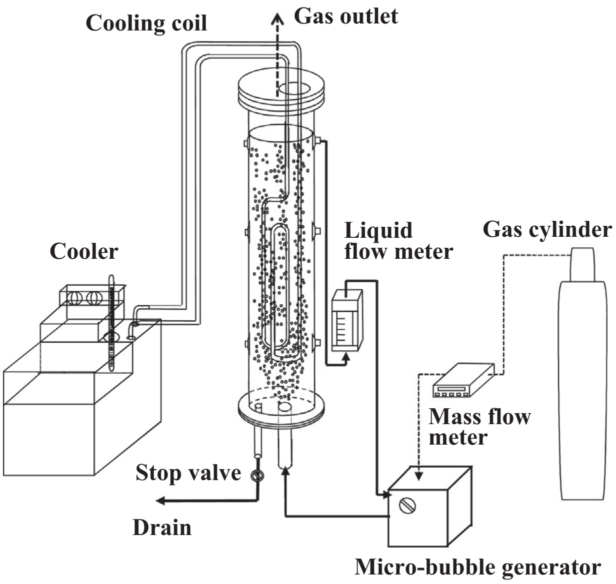

Fig. 1. Schematic diagram of the experimental apparatus.

Table 1
Experimental conditions.

Column inside diam. (m)	0.150			
Column height (m)	1.000	1.000	1.500	2.000
Liquid depth (m)	0.500	0.850	1.350	1.850
Superficial gas velocity × 10^4 (m/s)	0.944–6.61			
Superficial liquid velocity × 10^3 (m/s)	Mainly 9.44 (4.72–14.15)			
Water temperature (°C)	25 ± 0.1			